Advances in Nanochemistry
ISSN: 2676-5462

Research

Design and synthesis of magnetic MOF for the removal of erythrosine B dye using design of experiment

Vahid Noorzadeh, Hossein Peyman *

Department of chemistry, Ilam branch, Islamic Azad University, Ilam, Iran

Received 28th August 2021,
Accepted 29th September 2021,
DOI:10.22126/anc.2021.6871.1033

Abstract

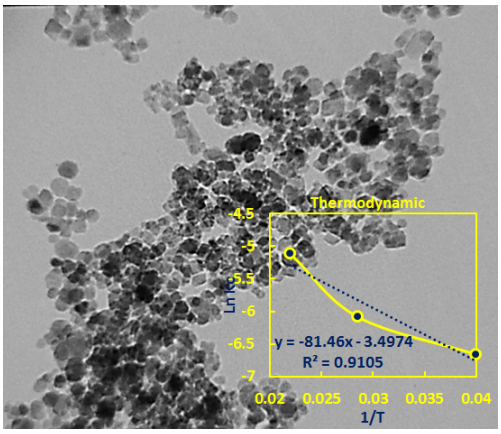

Dye and textile industries are suffering from pollutant issues from industrial wastewater. Due to attempts made by textile industries for producing diverse products, using different chemical compounds, especially new dyes, and creating complex wastewater are unavoidable. To date, various physical and chemical processes such as chemical precipitation, adsorption, electrocoagulation, etc. were used to treat relevant wastewater. Physicochemical systems such as surface adsorption have attained many interests, due to the unique physical and chemical properties of these nanoparticles compared to the balk type. Among different nanomaterials, magnetic nanomaterials were received the highest interest due to the facile separation by an external magnetic field and their high capacity. Iron oxide nanoparticles, specially super-magnetic or magnetic Fe_3O_4 nanoparticles, have the highest usage. Considering the specific properties of magnetic MOF, the physical and structural features of the synthesized adsorbent were investigated by BET, XRD, FTIR, SEM, and TEM techniques. The effect of different parameters such as pH, the concentration of erythrosine B dye, adsorbent weight, contact time, and the temperature was studied to determine the thermodynamic parameters, equilibrium isotherms, kinetic of the adsorption process, and finally their application on the adsorption of erythrosine B dye.

Keywords: *Metal-organic framework, Magnetic nanoparticle, Dye removal, Erythrosine B, Experimental design.*

Introduction

Dyes are an important pollutant that causes serious dangers for humans, animals, and other live objects. Dyes are not decomposed by anaerobic refinements, therefore, it is necessary that removes them from civil pollutants before releasing into the environment. Dyes are extensively used in textile, plastic, printing, etc. industries. To date, more than ten hundred types of commercial dyes were added to the market which is produced at the rate of 7 x 10^5 tons per year. Commonly, almost two percent of the produced dyes are released as wastewater to the environment, which is a significant volume. Dyes are counted as one of the main pollutants due to their various applications. A part of the light that enters the water is absorbed or reflected by dyes that stop the growth of healthy bacteria in water.[1-4] There are some technologies to remove dyes and other pollutants such as adsorption, coagulation, or separation, which are commercially available. However, they cannot completely convert the pollutants into less-toxic compounds or provide their biodegradation.

Other wastewater treatment methods such as chemical techniques and membrane usage are costly and produce new pollutants. For example, conventionally used chlorination produces carcinogenic materials and threatened human health.[5-7] In the recent decade, a variety of common methods such as physical methods, chemical oxidation, chemical coagulation, reverse osmosis, flocculation, biological treatment, electrochemical treatment, ion exchange, and surface adsorption were studied for the removal of the dye from wastewater, that they have differences in performance and environmental impacts.[8-9]

To decompose the organic pollutants, advanced oxidation processes containing Fenton, Senolysis, Ozonation, and the methods that are the combination of different techniques, have been extensively used. There are numerous reports on the usage of known semiconductors (e.g. ZnO, ZnS, etc.) as photocatalysts for oxidation processes. These nanoparticles can effectively play the catalyst role.[10-16] The application of these materials is associated

*Corresponding authors: Hossein Peyman, Email: hosseinpeyman@yahoo.com

Cite this article: Noorzadeh, V. & Peyman, H. (2021). Design and synthesis of magnetic MOF for the removal of erythrosine B dye using design of experiment. *Advances in Nanochemistry*, 3(2), 80-87. DOI: 10.22126/anc.2021.6800.1032

Publisher: Razi University

with some problems, which challenge their commercial usage. Difficult separation, agglomeration, and low quantum efficiency are some of their disadvantages that limit their commercial application. In recent years, wide researches on metal-organic frameworks have introduced a new category of photocatalysts.[17-20]

Metal-organic frameworks (MOFs) are a new category of inorganic compounds that have received many interests due to their high surface area, flexibility, design, and simple synthesis. These compounds have been used in different areas such as catalytic processes, separation, gas storage, adsorbent of different molecules, magnetic, and luminescence. These compounds are prepared by metallic ions or clusters and multidentate organic ligands to form a 3D structure.[21,22] An addition to the extraordinary properties of metal-organic frameworks is the photocatalytic effect that is applicable for organic pollutant removal. In recent years, investigations on metal-organic networks such as coordination polymers or structures with MOFs are highly regarded. Clusters of transition metal carboxylates are appropriate for the preparation of MOFs due to their application on bonding with organic linkers and creating extended frameworks with high stability and due to the nature of the networks and undemanding counter ions, as secondary building units (SBUs).[23]

Food colors are the chemicals used for food design. For centuries, humans added colors to their food. For years, hundreds of artificial food colors introduced, however, most of them are toxic. A rare number of them are still used in foods. The food industries often prefer artificial food colors rather than natural ones such as beta-carotene, beetroot extract, because they contain more attractive and shining colors.

There are still some discussions over the immunity of artificial food colors. All the artificial colors which currently are used in food, have passed different experiments about their toxicity. Regulatory agencies such as the United States Food and Drug Administration (FDA), and European Food Safety Authority have concluded that artificial food colors do not pose significant health risks. However, not everyone agrees with this conclusion. In this regard, some artificial food colors have been considered safe in one country, however, their human usage is forbidden. Therefore, the situation for their risk evaluation is complex. Erythrosine B, known as red 3, is the most controversial artificial food color. In a study, the male mice that received erythrosine B were at an increased risk for thyroid tumors. According to this research, FDA banned the erythrosine usage in 1990, although later stopped it. After some investigation, it was found that the thyroid tumors were not created by the direct effect of erythrosine.[24]

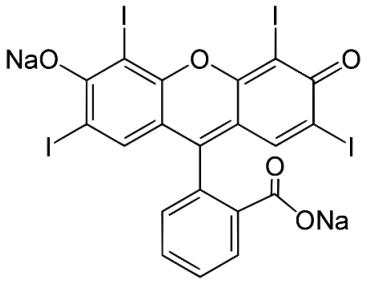

Scheme 1. *The structure of erythrosine B dye.*

An English scientist, called Fischer in the 1920s, first introduced the design of the experiment. With the use of the design of the experiment, the lowest number of experiments can achieve the most data about the under-study system. The design of the experiment provides the feasibility of determining the parameters, which have significant effects on the response. Furthermore, the interaction between parameters can be studied, a mathematical model can be proposed, and the optimum conditions for the interest system can be determined. The design of the experiment is a beneficial method that assists data evaluation and objective inference of analysis before the experiment runs. By running experimental designs, one can determine the optimum value of measurements (responses) or the conditions in which the inconsistent responses have good compatibility. In this work, magnetic MOF with iron oxide nanoparticles has been synthesized and used for the removal of erythrosine B dye. Minitab software and the Taguchi method were used for the determination of optimum conditions.

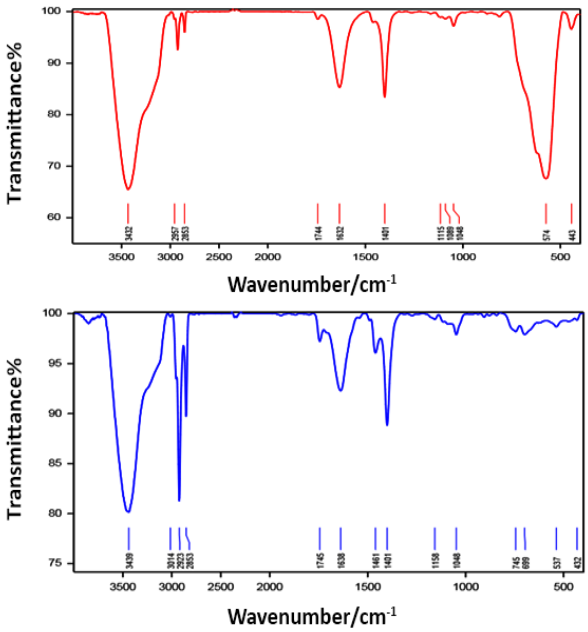

Figure 1. *FT-IR spectra of iron oxide nanoparticle and MOF.*

Experimental

Materials

The materials that have used in this research including iron(II) chloride tetrahydrate, iron(III) chloride hexahydrate, zinc chloride, hydrochloric acid, dimethyl formaldehyde, ammonia, ethanol, Erithsion B, sodium hydroxide and terephthalic acid are purchased from Merck company and used without further purification. For pH adjustment, sodium hydroxide and hydrochloric acids were used.

Instruments

Different instruments were used in this research which are listed in Table 1.

Table 1. *The list of the used instruments*

Instruments	Properties
Spectrophotometer	Two-beam Lambd 25
Ultrasonic	VGT-1730QTI
Hitter	IKA RH basic2
Microsampler (0.5-10 µL)	BOECO Germany
Microsampler (10-100 µL)	Sartorius
Balance	Sartorius
pH meter	Metrohm
Quartz cell	Q01104
Magnet	200 Tesla
Rotary	DRAGON LAB

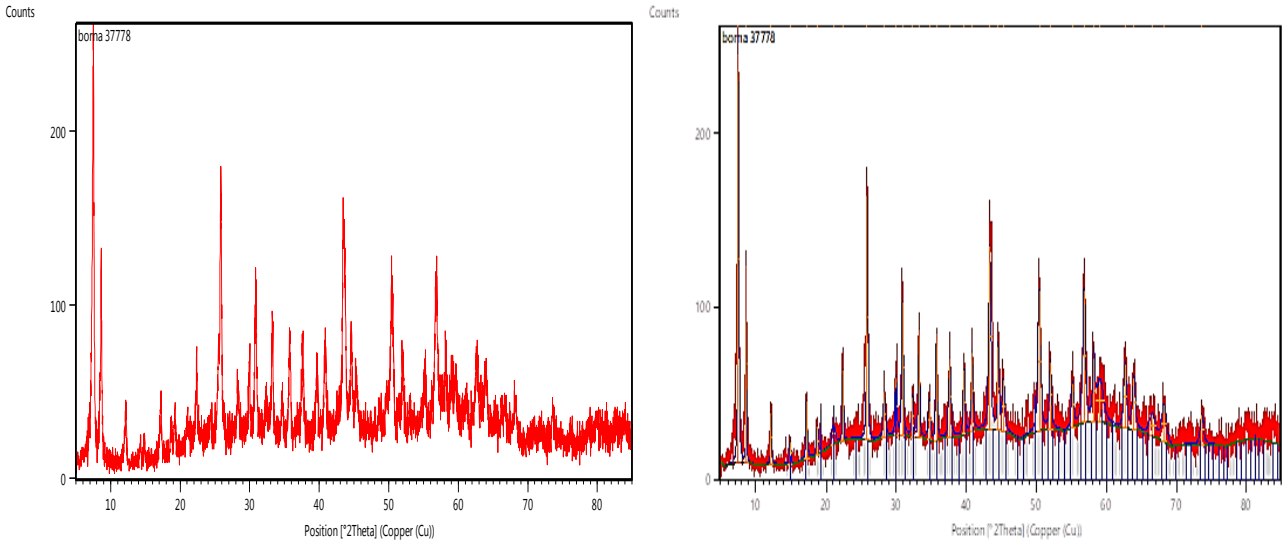

Figure 2. *The XRD spectrum of* ***(A)*** *the synthesized and* ***(B)*** *the reference MOF.*

Synthesis of iron oxide nanoparticle

To synthesis iron oxide, 5.2 g of $FeCl_3.6H_2O$ and 3.825 g $FeCl_2.4H_2O$ were added to the 25 mL deionized water. It was sonicated for 10 minutes and 25 mL of sodium hydroxide solution (1.5 M) was dropwise added until a suspension was achieved. Then, it was centrifuged at 4000 rpm for 30 minutes. The precipitants were transferred to a beaker and 100 mL deionized water was added to them. It was sonicated for a couple of minutes and a suspension was achieved. Further, it was centrifuged at 4000 rpm for 30 minutes. Rinsing was repeated three times and finally, the precipitants were transferred into 500 mL hydrochloric acid (0.01 M). Again, it was sonicated, then centrifuged and dried.

MOF preparation

First, 123 g $ZrCl_4$ was transferred to a beaker and 5 mL dimethyl formaldehyde was added to them. Then, 1 mL concentrated hydrochloric acid solution was added to them and was sonicated for 20 minutes. Next, 10 mL dimethyl formaldehyde and 134 g terephthalic acid were added to them. Then, the beaker was kept in an oven at 80 °C for 24 h. After centrifugation, two times, some amount of DMF was added to the precipitants and was sonicated for 5 minutes. Again it was centrifuged and the same process was repeated two times with ethanol. In the end, the final solution was transferred to the rotary at 90 °C under vacuum condition for 20 minutes. The MOF precipitants were achieved.

Preparation of magnetic MOF

For preparation of magnetic MOF, all the nanoparticle preparation steps were applied. However, first MOF were dispersed in deionized water, then, it was added to 5.2 g $FeCl_3.6H_2O$ and 3.825 g $FeCl_2.4H_2O$. The other steps were applied just as the preparation of nanoparticles.

Optimization of dye concentration

To determine the optimum amount of dye adsorption by magnetic MOF, the parameters of pH, temperature, dye concentration, and the magnetic MOF amount were applied just as in our previous studies. With the use of the design of the experiment in Minitab software and the Taguchi method, the experiment table (Table 2) with 27 different experiments was done to obtain the optimum mode for the highest dye removal.

After the design of the experiment, the experimental works were done. After each level, the amount of the adsorbed dye was measured by spectrophotometer and the value was compared with the same concentration of dye at the same pH in absence of magnetic MOF. The dye removal percentage was calculated by the absorption difference using equation 1:

$$\frac{A1-A2}{A1} \times 100 \quad (1)$$

After achieving the results and adding them to the Minitab software, the optimum conditions were achieved and further experiment steps were done in this condition and the adsorption isotherms were investigated.

Table 2. *Design of experiment with Minitab software for determination of optimum conditions.*

N	Adsorbent weight (mg)	Dye concentration (10^{-6} M)	Temperature (°C)	pH	Contact time (h)
1	0.5	1	25	3	1
2	1.2	1	25	3	1
3	2	1	25	3	1
4	0.5	5	35	7	1
5	1.2	5	35	7	1
6	2	5	35	7	1
7	0.5	10	45	9	1
8	1.2	10	45	9	1
9	2	10	45	9	1
10	0.5	10	35	3	12
11	1.2	10	35	3	12
12	2	10	35	3	12
13	0.5	1	45	7	12
14	1.2	1	45	7	12
15	2	1	45	7	12
16	0.5	5	25	9	12
17	1.2	5	25	9	12
18	2	5	25	9	12
19	0.5	5	45	3	24
20	1.2	5	45	3	24
21	2	5	45	3	24
22	0.5	10	25	7	24
23	1.2	10	25	7	24
24	2	10	25	7	24
25	0.5	1	35	9	24
26	1.2	1	35	9	24
27	2	1	35	9	24

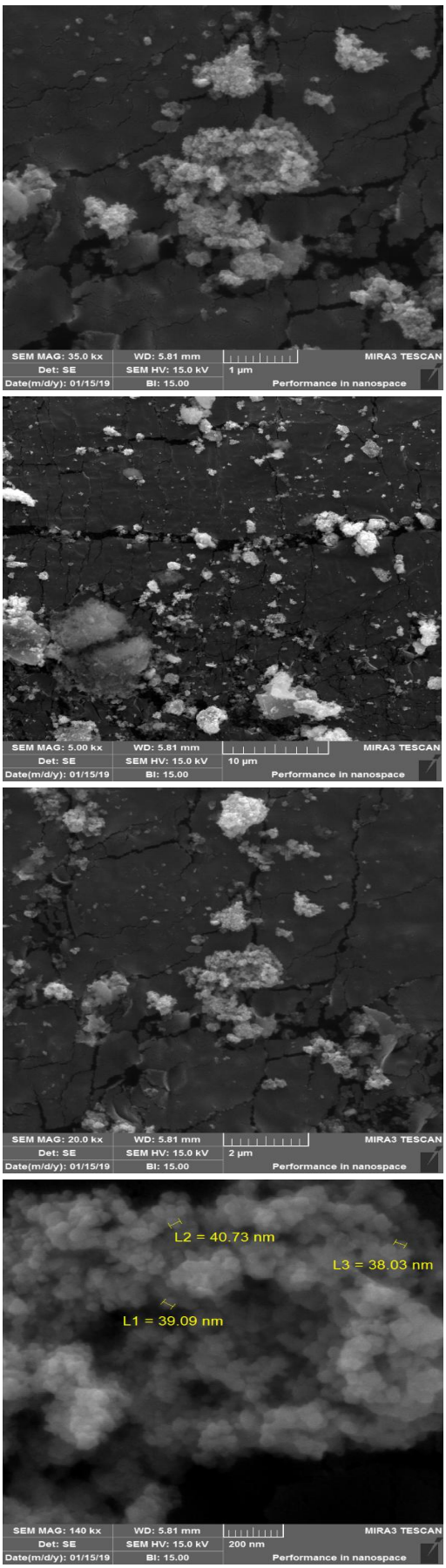

Figure 3. *The FESEM image of the synthesized MOF.*

Results and discussion

In this section, after the synthesis of nanoparticles, MOF, and magnetic MOF, they were characterized and studied by XRD, TEM, FT-IR, SEM, and BET techniques. Moreover, the results of choosing the best adsorbent and the used techniques for physical and chemical properties investigations are discussed. Then, the surface adsorption of erythrosine B dye on the adsorbent are studied from thermodynamic and kinetic points of view. In addition, the effect of different parameters such as temperature, dye concentration, time, adsorbent amount, and pH are investigated.

FT-IR analysis of Fe_3O_4 nanoparticle and MOF

To evaluate the synthesis of iron oxide (Fe_3O_4) nanoparticles, the FT-IR spectrum was recorded from the nanoparticles. It is known that the metallic nanoparticles have stretching vibration absorption peaks at lower wavenumbers of 1000 cm^{-1}, see Figure 1A. As shown in the figure, at the wavenumber of 574 cm^{-1}, there is a sharp stretching absorption peak of Fe-O. Moreover, there is another absorption peak in the region of 3432 cm^{-1} for the stretching vibration of the O-H bond in surface-adsorbed water molecules.

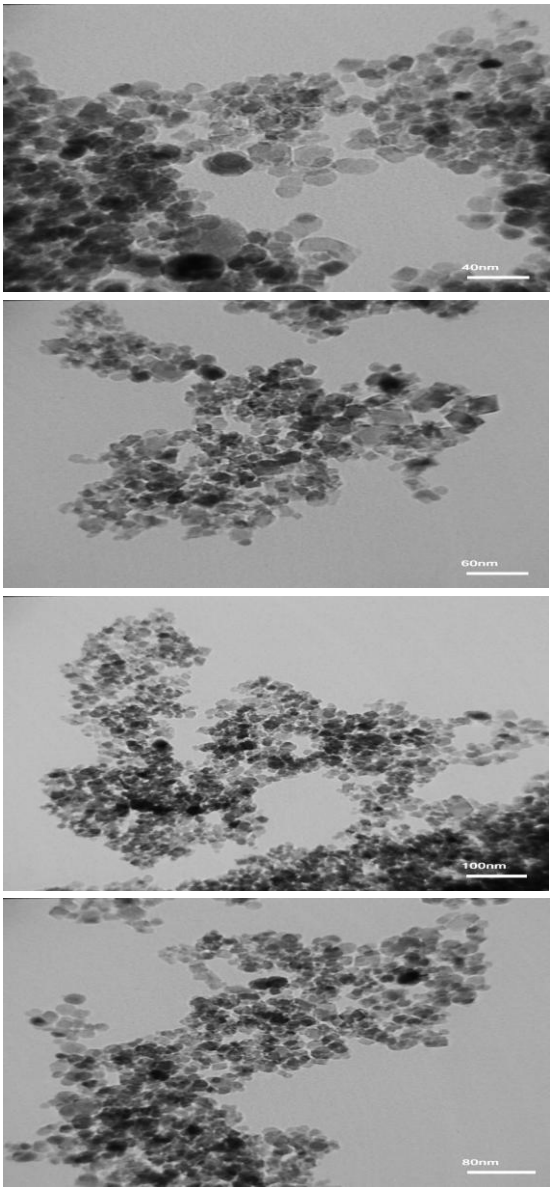

Figure 4. *TEM images of magnetic MOF in different magnifications.*

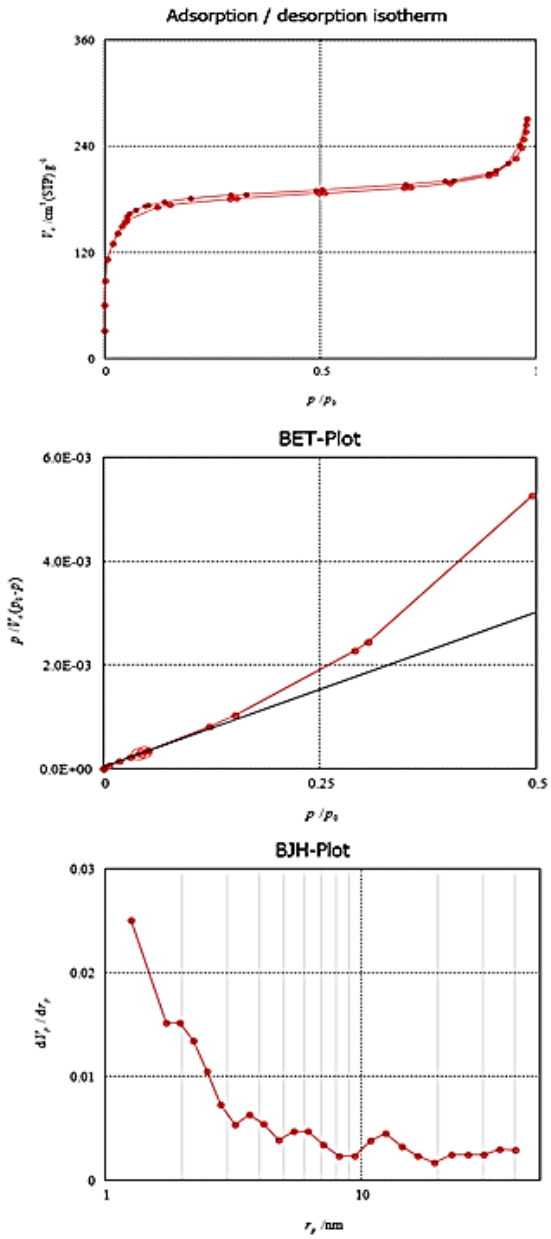

Figure 5. *The results of BET analysis on the synthesized MOF.*

The peaks at 1744 cm^{-1}, 1632 cm^{-1}, and 1401 cm^{-1} are related to the vibrations of C=O, C=C, and C-O groups, respectively.

To evaluate the synthesis of MOF, it was also studied by FT-IR spectroscopy. As shown in Figure 1B, the FT-IR spectrum of MOF has no sharp peaks at low wavenumbers of below 1000 cm^{-1}, which shows the absence of metallic nanoparticles. However, the peaks in the region of 1400 cm^{-1} are according to the vibrations of the O-C-O group. These peaks approve of the aromatic ring in the metal-organic structure. The peaks in the region of 3000 cm^{-1} are related to the C-H bond vibration in the aromatic ring.

XRD analysis of MOF

In order to characterize the MOF structure in the absence of magnetic nanoparticles, it was studied by the XRD technique, see Figure 2A. As shown in Figure 2A, the XRD spectrum contains many sharp peaks for the synthesized MOF which accord the reference XRD spectrum of cubic MOF in Figure 2B.

FESEM images of MOF

The SEM images of MOF are presented in Figure 3, in which the synthesized MOF has a size distribution of 1-50 nm, with an average size of 38.5 nm.

The TEM images of magnetic MOF

The TEM images of the magnetic MOF is presented in Figure 4. Both magnetic iron oxide nanoparticles and MOF are obvious in the Figure 4.

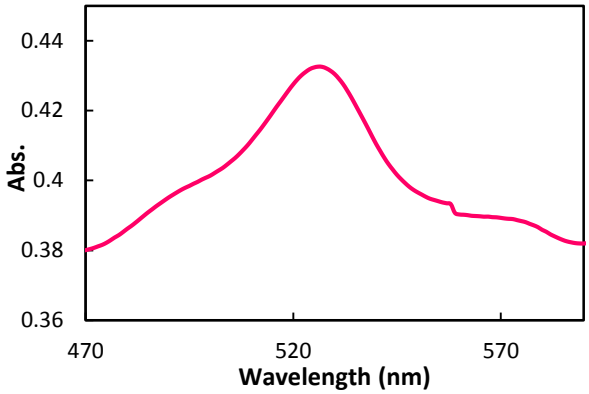

Figure 6. *The absorption spectrum of erythrosine B dye.*

BET analysis of MOF

BET analysis is an effective technique to study adsorbents. To determine the effective surface area of the synthesized MOF, it was studied by the BET method under nitrogen gas, see Figure 5. As shown in Figure 5A, the adsorption spectrum of MOF was recorded under nitrogen gas, which shows the type-2 isotherm of non-porous compounds as adsorbents. Figure 5B shows the effective surface of the adsorbent. According to this result, every gram of the synthesized MOF contains an effective surface area of 166.94 m^2. By means of BET analysis, one may also receive information about the nanoparticles size or the average size of the under-study material. According to Figure 5C, the synthesized MOF has the size range of 1-50 nm and the average internal diameter of their cells is 1.26 nm.

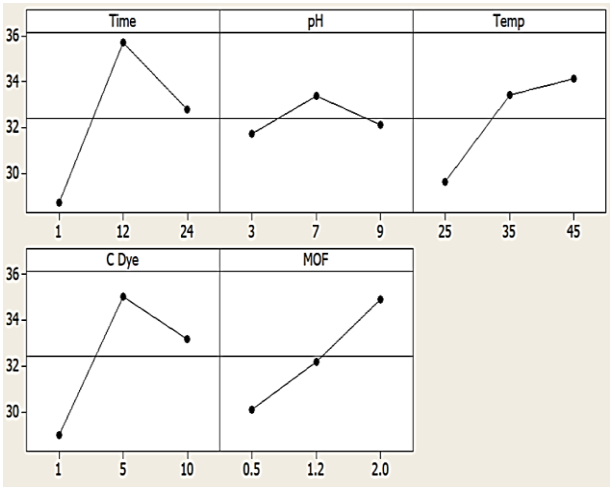

Figure 7. *The optimum conditions of the removal of the erythrosine B dye.*

The absorption spectrophotometry of erythrosine B dye

In this research the removal of erythrosine B dye was investigated. In this regard, the UV-Vis absorption spectrum of erythrosine B dye was recorded. In Figure 6, the dye has a maximum absorption peaks at the wavelength of 526 nm, as the maximum absorption wavelength of erythrosine B dye in further experiments.

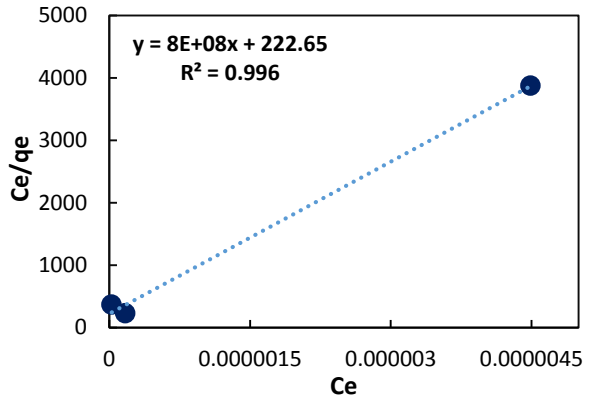

Figure 8. *The Langmuir adsorption isotherm.*

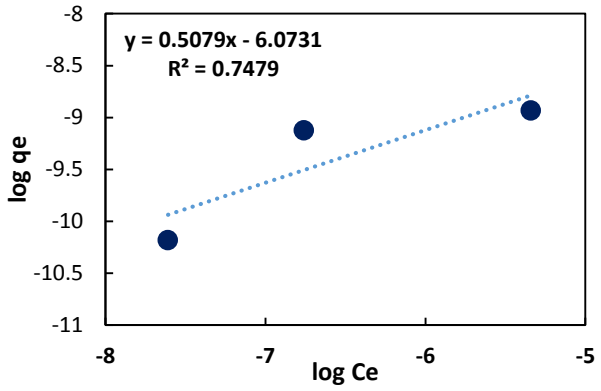

Figure 9. *The Freundlich adsorption isotherm.*

The optimization of the removal conditions

To study the optimum conditions for the removal of erythrosine B dye by magnetic MOF adsorbent, 27 experiments were defined for different parameters of temperature, dye concentration, contact time, pH, and adsorbent amount in the Minitab software with Taguchi mode. By running these experiments, calculating the removal ratio for each condition, and loading the results into the Minitab software, the optimum condition was obtained as Figure 7. The optimum contact time is 12 h, the temperature is 45 °C, the dye concentration is 5 x 10^{-6} M, pH is 7, and the absorbent weight is 2 mg. For the evaluation of the optimum conditions, the dye removal experiment was repeated in the same condition, in which the results showed a suitable validity of 95%.

The comparison of dye removal by magnetic and non-magnetic adsorbents

The erythrosine B dye removal was studied by both MOF and magnetic MOF under the optimum condition. The results show a difference of the removal in the presence of two different adsorbents. In the same conditions, the magnetic adsorbent had the positive effect on the dye removal (Table 3).

Table 3. *The difference in the results of erythrosine B dye removal by the magnetic MOF and MOF under optimum condition.*

N	Dye concentration (-log C) (M)	Difference in dye removal between magnetic MOF and MOF
C1	6	2.89
C2	5.3	6.23
C3	8	8.33
C4	7.3	9.48

Adsorption isotherm

For each dye solution, the value of q_e (see equation 2) and adsorption were calculated and the isotherm diagrams were plotted.

$$q_e = \frac{C0-Ce}{M} \times v \quad (2)$$

Langmuir adsorption isotherm

Langmuir adsorption isotherm is an adsorption mechanism of adsorbate on the surface of the adsorbent that follows equation 3. The plot of $\frac{C_e}{q_e}$ versus C_e was drawn, which has R^2 = 0.996 (Figure 8).

$$\frac{C_e}{q_e} = \frac{1}{q_m \ k_1} + \frac{C_e}{q_m} \quad (3)$$

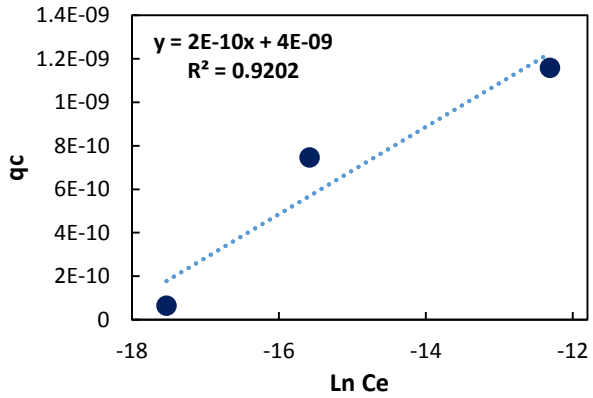

Figure 10. *The Temkin adsorption isotherm.*

Freundlich adsorption isotherm

The Freundlich adsorption isotherm is according to equation 4.

$$\log q_e = \log k_f + \frac{1}{n_f} \log c_e \quad (4)$$

Where, q_e is the equilibrium amount of adsorbate, k is the equilibrium constant, k_f and n_f are Freundlich constants where are the intensity of the surface adsorption and the capacity of the surface adsorption, respectively. Log q_e versus log C_e is plotted in Figure 9.

Temkin adsorption isotherm

Temkin adsorption isotherm follows equation 5. By plotting q_e versus ln C_e in Figure 10, R^2 = 0.9202 was achieved.

$$q_e = \log k_t + \ln c_e \quad (5)$$

According to different R^2 values for Langmuir, Freundlich, and Temkin isotherms, one may conclude that the adsorption mechanism of erythrosine B dye on the surface of magnetic MOF adsorbent is the Langmuir type.

Adsorption kinetic

The adsorption kinetic of erythrosine B dye on the surface of magnetic MOF accords the first-order (equation 6) and second-order (equation 7) equations.

$$\log(q_e - q_t) = \log q_e - \frac{k_1}{2.33} t \quad (6)$$

$$\frac{t}{q_t} = \frac{1}{k_e q_e^2} - \frac{1}{q_t} t \quad (7)$$

In the first-order kinetic, by plotting $\log(q_e - q_t)$ versus t, R^2 = 0.5802 has achieved (Figure 11A). In Figure 11B, the second-order kinetic diagram was plotted as $\frac{t}{q_t}$ versus t by R^2 = 0.994. The results show this study is following the second-order kinetic.

Adsorption thermodynamic

The adsorption of erythrosine B dye on the surface of the magnetic adsorbent was studied in different temperatures of 25, 35, and 45 °C in the presence of adsorbent. Equations 8 and 9 were used to calculate enthalpy ΔH° and entropy ΔS°.

$$kc = \frac{q_e}{c_e} \quad (8)$$

$$\ln kc = \frac{\Delta S^\circ}{R} - \frac{\Delta H^\circ}{RT} \quad (9)$$

According to the calculated results, ΔH° = - 677.258 kJ and ΔS°= -29.077 kJ were achieved.

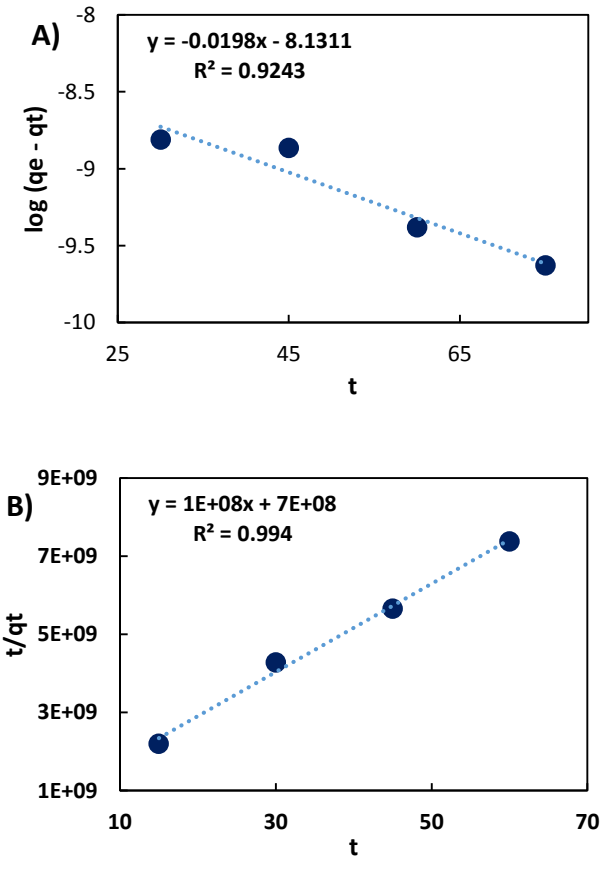

Figure 11. *The dye adsorption kinetic by* ***(A)*** *first-order and* ***(B)*** *second-order equations.*

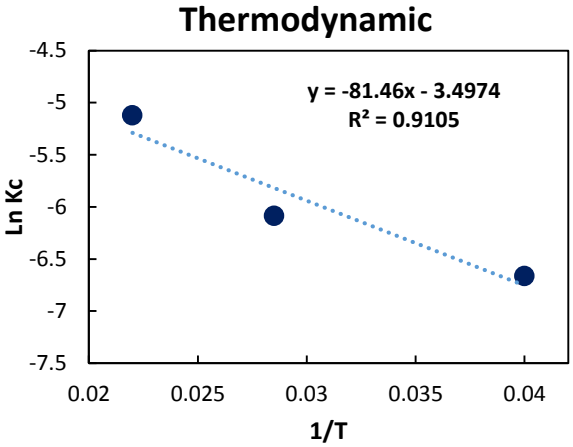

Figure 12. *The thermodynamic of dye adsorption on the surface of adsorbent.*

Conclusion

In this work, the separation of the nano-adsorbent was applicable by an external magnetic field due to the use of magnetic iron oxide nanoparticles. The synthesized materials were studied by FT-IR, FESEM, TEM, BET, and XRD techniques. The results show that the removal of the erythrosine B dye was successfully done by the proposing magnetic MOF adsorbent. The optimum conditions were achieved by the design of the experiment in Minitab software, which are the contact time of 12 h, the temperature of 45 °C, dye concentration of 5 x 10^{-6} M, pH 7, and adsorbent weight of 2 mg. The kinetic, thermodynamic, and adsorption isotherm studies were done. The adsorption isotherm of erythrosine B dye on the surface of adsorbent is as Langmuir type and contains the second-order kinetic. The thermodynamic parameters have also shown the appropriate adsorption process.

References

1. C. Biondi, M. Bonamico, L. Torelli, and A. Vaciago, *Chem. Commun.*, 10, **1965**, 191.
2. H.A. Modi, G. Rajput, and C. Ambasana, *Bioresour. Tech.*, 101, **2010**, 6580.
3. G. Crini, *Bioresour. Technol.*, 97, **2006**, 1061.
4. A. Mittal, A. Malviya, D. Kaur, J. Mittal, and L. Kurup, *J. Hazard. Mater.*, 148, **2007**, 229.
5. S. Chen, J. Zhang, C. Zhang, Q. Yue, Y. Li, and C. Li, *Desalination*, 149, **2010**, 252.
6. Q. Qin, J. Ma, and K. Liu, *J. Hazard. Mater.*, 162, **2009**, 133.
7. U. I. Gaya and A. H. Abdullah, *J. Photochem.C. Photobiol.*, 1, **2008**, 9.
8. S. Wang, *Dyes Pigm.*, 76, **2008**, 714.
9. V. Prigione, G.C. Varese, L. Casieri, and V.F. Marchisio, *Bioresour. Technol.*, 99, **2008**, 3559.
10. D. Wang, T. Silbaugh, R. Pfeffer, and Y. Lin, *Powder Technol.*, 203, **2010**, 298.
11. D. Lin, Q. Zhao, L. Hu, and B. Xing, *Chemosphere.*, 103, **2014**, 188.
12. M.N. Chong, B. Jin, C.W. Chow, and C. Saint, *Water Res.*, 44, **2010**, 2997.
13. D.H. Bremner, R. Molina, F. Martínez, J.A. Melero, and Y. Segura, *Appl. Catal. B*, 90, **2009**, 380.
14. M.I. Litter, *Appl. Catal. B*, 23, **1999**, 89.

15. K. Nakata and A. Fujishima, *J. Photochem. Photobiol. C*, 13, **2012**, 39.
16. A. Janczyk, E. Krakowska, G. Stochel and W. Macyk, *J. Am. Chem. Soc*., 128, **2006**, 15574.
17. A. Hajesmaili and Z. Bahrami, *J. Appl. Chem*., 11, **2017**, 91.
18. U. Akpan and B. Hameed, *J. Hazard. Mater*., 170, **2009**, 520.
19. K. Ayoub, E. D. van Hullebusch, M. Cassir and A. Bermond, *J. Hazard. Mater*., 10, **2010**, 178.
20. A. Mills and S. Le Hunte, *J. Photochem. A. Photobiol*., 1, **1997**, 180.
21. J. Lu, J.X. Lin, X.L. Zhao and R. Cao, *Chem. Commun*., 48, **2012**, 669.
22. H. Yang and H. Cheng, *Sep. Purif. Technol*., 56, **2007**, 392.
23. A. Leonard, P. J. Reucroft, and G.B. Freeman, Gas adsorption by activated and impregnated carbons. US Army Armament Research and Development Command Chemical Systems Laboratory Jonas Chemical Laboratory, Edgewood Arsenal, Aberdeen Proving Ground, Maryland (1977) 21010.
24. O. Hiasa, M. Ohshima, Y. Kitahori, N. Konishi, T. Shimoyama, Y. Sakaguchi, H. Hashimoto, S. Minami, and Y. Kato, *Jpn. J. Cancer Res*., 79, **1988**, 314.